End Effects of Rare Gas Flow in Short Channels and in Squeezed-Film Dampers

Timo Veijola

Department of Electrical and Communications Engineering,
Helsinki University of Technology,
P.O.Box 3000, FIN-02015 HUT, Finland, timo.veijola@hut.fi

ABSTRACT

Simple approximate design formulas (±5%) are presented for calculating the elongation of the idealized viscous flow channel of rare gas at Knudsen numbers $K_n < 100$ due to the open end effects. Rectangular channels with a large aspect ratio and circular channels are discussed. The elongation model is applied to a squeezed-film damper problem and a simple design formula is presented that approximates the end effects in the damper.

Keywords: End Effect, Rarefied Gas Flow, Compact Model, Squeezed-Film Damper, Knudsen Number

1 INTRODUCTION

Gas rarefaction plays an important role in predicting the damping in micromechanical structures, especially when the characteristic dimensions are small and when the gas pressure is low. The measures for gas rarefaction are both the Knudsen number $K_n = \lambda/d$, and the inverse Knudsen number $D = \sqrt{\pi}/2/K_n$, where λ is the mean free path of the gas, inversely proportional to pressure, and d is the characteristic dimension of the flow channel.

Models for viscous gas flow in long rectangular and circular channels at any values of K_n are well known [1]. But for short channels, where the channel length is comparable with its height, general models do not exist. Models have been presented for rectangular channels only in the molecular flow regime [2], [3], and models valid at any K_n have been presented only for circular channels [1] and rectangular channels with an infinite aspect ratio [1].

The first part of this paper presents simple approximate design formulas for calculating the elongation of the idealized viscous flow channel of rare gas due to the open end effects.

A compact squeezed-film damper model has been presented for cases where the gap height is very small compared with the surface dimensions [4], [5]. This idealized model underestimates the damping force, since the fringe effects at the surface borders are ignored. Vemuri et al. [6] showed by 3D flow simulations and measurements that the fringe effects considerably increase the damping force (35 %), even at surface width / gap height ratios of 20. In [7] we have presented an analytic compact model that includes the effects of the borders, based on the analytic solution of the Reynolds equation [8].

The second part of this paper presents a correction to our previous model [7], and the model is extended further to include the effect of rare gas, utilizing the results presented in the first part of this paper.

2 GAS FLOW IN SHORT CHANNELS

Let us study the slowly oscillating (Reynolds number $\mathrm{Re} \ll 1$) viscous flow of rare gas in short channels, Fig 1. The relative channel length L is $L_{ch} = a/d$ for a rectangular channel, and $L_{tb} = a/r$ for a circular channel. The channel length a is assumed to be much smaller than the acoustic wavelength. A small relative pressure difference $(p_2 - p_1)/p_1$ across the channel and isothermal conditions are assumed, as well.

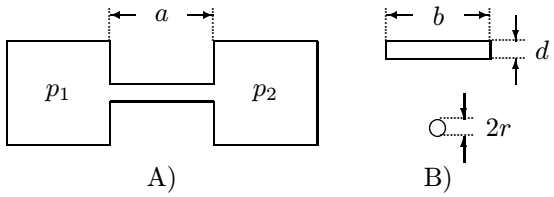

Figure 1: A) Flow channel between two gas reservoirs and B) the channel cross-sections.

The flow conductance is characterized by the Poiseuille flow rates $Q_{p,ch}(D_{ch})$ and $Q_{p,tb}(D_{tb})$ for rectangular and circular channels, respectively. $D_{ch} = d\sqrt{\pi}/2/\lambda$ and $D_{tb} = r\sqrt{\pi}/2/\lambda$ are the respective inverse Knudsen numbers. The flow rate of an infinitely long channel in the continuum flow regime is $Q_{p,ch}(D_{ch}) = D_{ch}/6$ for a rectangular channel with an infinite aspect ratio and $Q_{p,tb}(D_{tb}) = D_{tb}/4$ for a circular channel. The contribution of the flow rate can be included in the viscosity coefficient η by specifying the effective viscosity as

$$\eta_{\mathrm{eff}} = \eta \frac{Q_p(\infty)}{Q_p(D)}. \quad (1)$$

This effective viscosity model is valid for infinite L. In short channels, the flow rate is affected also by the fringe flow when the gas enters the channel and escapes from it. Here, it is assumed that this change in the flow rate can be modelled with an additional flow conductance $G_{\rm end}$ at the channel ends

$$G(L) = G(\infty) + G_{\rm end}, \tag{2}$$

instead of including the end effects in the effective viscosity. This additional flow conductance $G_{\rm end}$ is modelled here with a relative elongation $\Delta L(D, L)$ of the channel. The flow rate of the finite channel can be written as

$$Q_{\rm p}(D, L) = \frac{L}{L + \Delta L(D, L)} Q_{\rm p}(D). \tag{3}$$

This equation is valid for any channel cross-section. In the following, rectangular channels (ch) and circular tubes (tb) are discussed.

2.1 Rectangular Channel With an Infinite Aspect Ratio

Sharipov and Seleznev [1] have calculated values for the flow rate from the Boltzmann equation for certain values of $D_{\rm ch}$ and $L_{\rm ch}$. The flow rate for infinite $L_{\rm ch}$ is approximated with [5] ($D_{\rm ch} > 10^{-3}$)

$$Q_{\rm p,ch}(D) \approx \frac{D}{6}(1 + 9.638 K_{\rm n}^{1.159}) = \frac{D}{6} + \frac{1.396}{D^{0.159}}. \tag{4}$$

Our novel approximation for the relative elongation is

$$\Delta L_{\rm ch}(D, L) \approx \frac{8}{3\pi} \frac{1 + 2.471 D^{-0.659}}{1 + 0.5 D^{-0.5} L^{-0.238}}. \tag{5}$$

Figure 2 shows $\Delta L_{\rm ch}$ as a function of the inverse Knudsen number $D_{\rm ch}$. In the slip and continuum flow regimes ($D_{\rm ch} > 10$), the relative elongation is nearly constant and independent of $L_{\rm ch}$. In the transitional and molecular flow regimes ($D_{\rm ch} < 10$), the relative channel elongation is larger, and depends on $L_{\rm ch}$. The flow rate $Q_{\rm p,ch}$ in Eq. (3) is drawn in Fig. 3 as a function of $D_{\rm ch}$ at five values of $L_{\rm ch}$. The approximation is compared with the published flow rate data [1]. The relative deviation is smaller than $\pm 5\%$.

According to Eq. (1), the effective viscosity is

$$\eta_{\rm eff,ch} = \frac{D_{\rm ch}\eta}{6 Q_{\rm p,ch}(D_{\rm ch})} \approx \frac{\eta}{1 + 9.638 K_{\rm n,ch}^{1.159}}, \tag{6}$$

and the resulting mechanical impedance of a channel of width b is

$$Z_{\rm m,ch} = 12 \eta_{\rm eff,ch} b [L_{\rm ch} + \Delta L_{\rm ch}(D_{\rm ch}, L_{\rm ch})]. \tag{7}$$

Since Re $\ll 1$ was assumed, the frequency-dependent part of the impedance due to the gas mass [9] is ignored here.

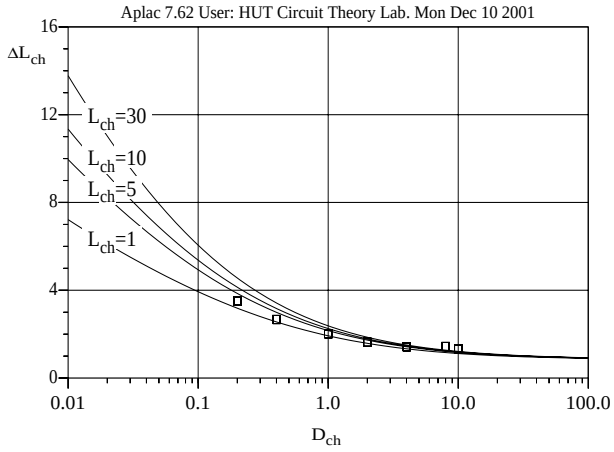

Figure 2: Relative elongation $\Delta L_{\rm ch}$ of the rectangular channel in Eq. (5) as a function of the inverse Knudsen number $D_{\rm ch}$ (——) and the results in [1] (□).

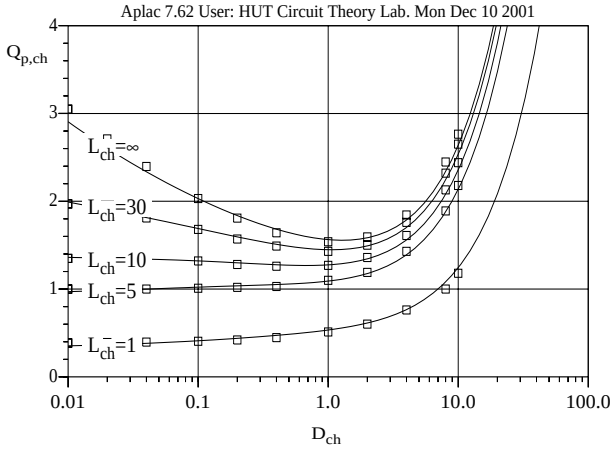

Figure 3: Flow rate coefficient $Q_{\rm p,ch}$ as a function of the inverse Knudsen number $D_{\rm ch}$ at $L_{\rm ch} = 1$, 5, 10, 30, and ∞ (——), and numerical results in [1] (□).

2.2 Circular Channel

Knudsen presented an approximate function for the flow conductance in long capillaries a hundred years ago. Here we present an equivalent approximation, fitted to the results solved from the Boltzmann equation [1] ($0 < D < \infty$):

$$Q_{\rm p,tb}(D) \approx \frac{D}{4} + 1.485 \frac{1.78D + 1}{2.625D + 1}, \tag{8}$$

where $D = D_{\rm tb}$. The relative channel elongation due to the finite length has been derived by fitting Eq. (3) to the flow rate coefficients given in [1], resulting in

$$\Delta L_{\rm tb}(D, L) \approx \frac{3\pi}{8} \frac{1 + 1.7 D^{-0.858}}{1 + 0.688 D^{-0.858} L^{-0.125}}. \tag{9}$$

The relative deviation of this approximation is less than $\pm 2\%$. Figure 4 shows $\Delta L_{\rm tb}$ as a function of $D_{\rm tb}$ at four

values of $L_{\rm tb}$. The relative channel elongation is almost constant and independent of L in the slip and continuum flow regimes ($D_{\rm tb} > 10$). In the transitional and molecular regimes ($D_{\rm tb} < 10$), it is larger, but saturates at $D_{\rm tb} < 0.1$. Figure 5 shows the flow rate coefficient for a circular channel as a function of $D_{\rm tb}$ for five values of $L_{\rm tb}$.

According to Eq. (1) the effective viscosity is

$$\eta_{\rm eff,tb} = \frac{D_{\rm tb}\eta}{4Q_{\rm p,tb}(D_{\rm tb})}, \tag{10}$$

and the resulting mechanical impedance of the tube is

$$Z_{\rm m,tb} = 8\pi\eta_{\rm eff,tb} r[L_{\rm tb} + \Delta L_{\rm tb}(D_{\rm tb}, L_{\rm tb})]. \tag{11}$$

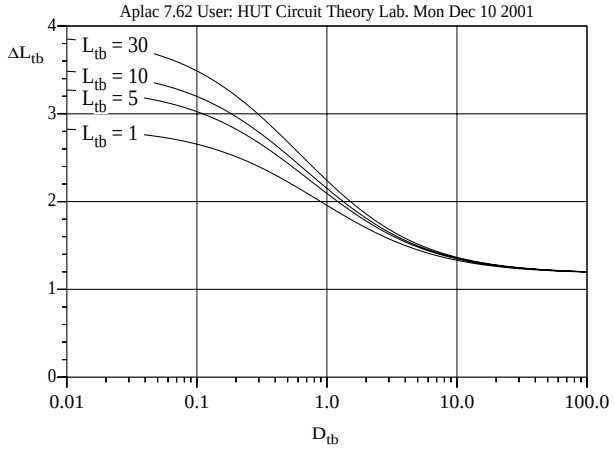

Figure 4: Relative elongation $\Delta L_{\rm tb}$ of the circular channel, Eq. (9), as a function of the inverse Knudsen number $D_{\rm tb}$.

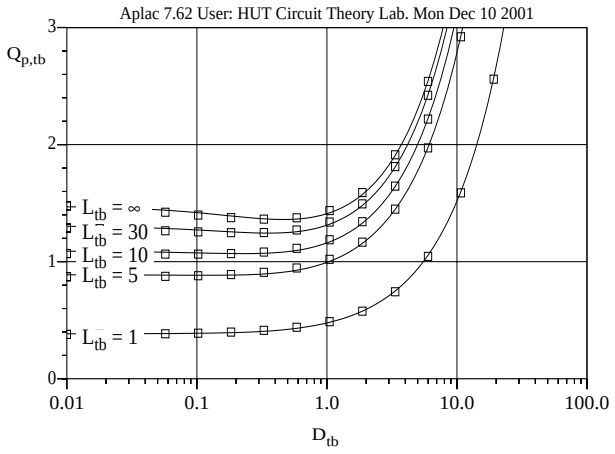

Figure 5: Flow rate coefficient $Q_{\rm p,tb}$ as a function of the inverse Knudsen number $D_{\rm tb}$ at $L_{\rm tb} = 1$, 5, 10, 30, and ∞ (——) and the results in [1] (□).

3 END EFFECTS IN SQUEEZED-FILM DAMPERS

Gas flow between two perpendicularly moving surfaces is very similar to the flow in channels. The elongation model for a rectangular channel in Eq. (5) is usable in calculating the end effect at the borders of a squeezed-film damper. However, in this case the elongation cannot be directly added to the damper dimension as in the capillary flow. The end effects are modelled here with lumped flow conductances at the borders, according to Eq. (2). This assumption is not accurate for small L, since the flow conductance in the gap varies close to the damper borders. Figure 6 shows the dimensions of a squeezed-film damper.

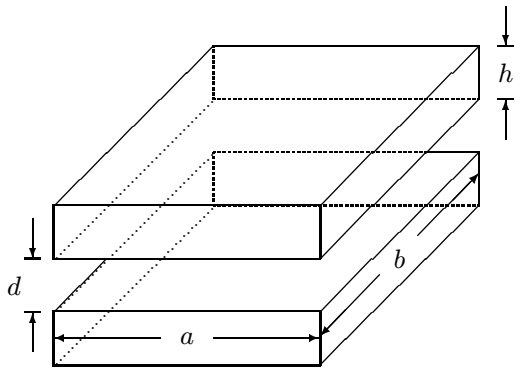

Figure 6: Dimensions of a squeezed film damper. The plate height h is assumed infinite here. The surfaces move perpendicularly causing fluid flow between them.

In [8], the squeezed-film damping problem has been solved analytically for rectangular, perpendicularly moving surfaces, including the acoustic conditions at the borders. The resulting mechanical admittance $Y_{\rm m}$ has been presented in [7] both as a complete, accurate equation and as a simplified approximation. The simplified model is:

$$Y_{\rm m} = \frac{1}{R_{1,1} + j\omega L_{1,1}}, \tag{12}$$

where the values for $R_{1,1}$ and $L_{1,1}$ are

$$R_{1,1} = \frac{\pi^6 d^3}{768\eta_{\rm eff,ch} a_0 b_0}\left(\frac{1}{a_0^2} + \frac{1}{b_0^2}\right), \tag{13}$$

$$L_{1,1} = \frac{\pi^4 d}{64 a b P_{\rm A}}, \tag{14}$$

where $\eta_{\rm eff,ch}$ is the effective viscosity given in Eq. (6) and $P_{\rm A}$ is the pressure, and $a_0 = a + \Delta a_{\rm s}$ and $b_0 = b + \Delta b_{\rm s}$ include the elongations. Note that the value of $L_{1,1}$, that models the compressibility of the gas, is not affected by the end effects.

3.1 Corrected End-Effect Model

First-order approximations for a_0 and b_0 are [7]

$$a_0 = a + \Delta a_\mathrm{s} = a\frac{\sqrt{1+3A_\mathrm{a}}\,(1+4A_\mathrm{b})^{3/8}}{\sqrt{1+3A_\mathrm{b}}\,(1+4A_\mathrm{a})^{1/8}}, \qquad (15)$$

$$b_0 = b + \Delta b_\mathrm{s} = b\frac{\sqrt{1+3A_\mathrm{b}}\,(1+4A_\mathrm{a})^{3/8}}{\sqrt{1+3A_\mathrm{a}}\,(1+4A_\mathrm{b})^{1/8}}, \qquad (16)$$

Values for A_a and A_b were derived incorrectly from the attached mass end correction in [7], since they are not valid for Re $\ll 1$. The end correction due to the viscous flow is used here instead.

In the pressure boundary conditions for the Reynolds equation [8], the values of $\nabla p/p$ at the borders are needed. Assuming that the pressure drops linearly at rate ∇p to zero at distance $\Delta a/2$ outside the damper borders, we can write $\nabla p \Delta a/2 = p$ at the borders. The corrected values for the coefficients A_a and A_b now depend on ΔL_ch in Eq. (5) and become

$$A_\mathrm{a} = \frac{\Delta a}{a} = \frac{\Delta L_\mathrm{ch}(D_\mathrm{ch}, L_\mathrm{a})}{L_\mathrm{a}}, \qquad (17)$$

$$A_\mathrm{b} = \frac{\Delta b}{b} = \frac{\Delta L_\mathrm{ch}(D_\mathrm{ch}, L_\mathrm{b})}{L_\mathrm{b}}, \qquad (18)$$

where $L_\mathrm{a} = a/d$ and $L_\mathrm{b} = b/d$.

3.2 Verification

The response of the corrected compact model was compared with the results of Vemuri et al. [6]. The relative effective increase $\Delta a_\mathrm{s}/d$ of the length is illustrated in Fig 7 ($a = b$) as a function of the aspect ratio $L_\mathrm{a} = L_\mathrm{b}$. The model gives slightly smaller values than the ones reported in [6]. This deviation is probably due to the fact that the gas cannot escape downwards from the aperture in the structure in [6], effectively increasing the elongation.

4 CONCLUSIONS

Simple models for rare gas flow conductances of short circular channels and rectangular slots were given. It was shown that the gas rarefaction makes the end effects even more important in the molecular and transitional flow regimes than in the continuum flow regime. The models are valid for $K_\mathrm{n} < 100$ with an accuracy of 5 %.

The elongation model for a rectangular channel was utilized in the squeezed-film damper problem assuming that the end effects can be presented as lumped flow conductances at the damper borders. A simple design equation calculating the mechanical admittance of the damper was given. It is valid for $K_\mathrm{n} < 100$, but its accuracy is not known for large K_n and small L. This new model is always more accurate than the old idealistic model [4], [5], especially when the surface width / gap height ratio is below about 20.

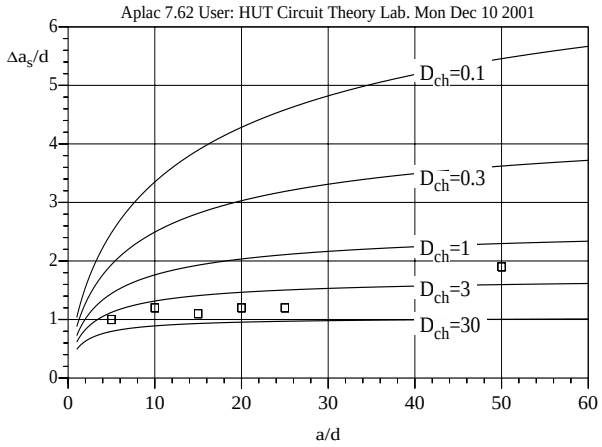

Figure 7: Relative elongation $\Delta a_\mathrm{s}/d$ in a squeezed-film damper as a function of the aspect ratio $L_\mathrm{a} = L_\mathrm{b} = a/d$ of the novel model (——) at five values of D_ch. The results in [6] are also shown (□) ($D_\mathrm{ch} \approx 30$).

REFERENCES

[1] F. Sharipov and V. Seleznev, "Data on Internal Rarefied Gas Flows," *J. Phys. Chem. Ref. Data*, vol. 27, no. 3, pp. 657–706, 1998.

[2] P. Y. Wang and E. Y. Yu, "Nearly Free-Molecular Channel Flow at Finite Pressure Ratio," *The Physics of Fluids*, vol. 15, no. 6, pp. 1004–1009, 1971.

[3] W. Steckelmacher, "The Effect of Cross-Sectional Shape on the Molecular Flow in Long Tubes," *Vacuum*, vol. 28, no. 6/7, pp. 269–275, 1979.

[4] W. S. Griffin, H. H. Richardson, and S. Yamanami, "A Study of Fluid Squeeze-Film Damping," *Journal of Basic Engineering, Trans. ASME*, pp. 451–456, June 1966.

[5] T. Veijola, H. Kuisma, J. Lahdenperä, and T. Ryhänen, "Equivalent Circuit Model of the Squeezed Gas Film in a Silicon Accelerometer," *Sensors and Actuators A*, vol. 48, pp. 239–248, 1995.

[6] S. Vemuri, G. K. Fedder, and T. Mukherjee, "Low-Order Squeeze Film Model for Simulation of MEMS Devices," *MSM'2000*, (San Diego), pp. 205–208, April 2000.

[7] T. Veijola, K. Ruokonen, and I. Tittonen, "Compact Squeezed-Film Damping Model Including the Open Border Effects," *Proceedings of MSM 2001*, (Hilton Head), pp. 76–79, April 2001.

[8] R. B. Darling, C. Hivick, and J. Xu, "Compact Analytical Modeling for Squeeze Film Damping with Arbitrary Venting Conditions Using a Green's Function Approach," *Sensors and Actuators A*, vol. 70, pp. 32–41, 1998.

[9] T. Veijola, "Acoustic Impedance Elements Modeling Oscillating Gas Flow in Micro Channels," *Proceedings of MSM 2001*, (Hilton Head), pp. 96–99, April 2001.